Topics in Catalysis (2019) 62:838–848
https://doi.org/10.1007/s11244-019-01163-4

ORIGINAL PAPER

Atomic Layer Deposition (ALD) as a Way to Prepare New Mixed-Oxide Catalyst Supports: The Case of Alumina Addition to Silica-Supported Platinum for the Selective Hydrogenation of Cinnamaldehyde

Zhihuan Weng[1] · **Francisco Zaera**[1,2]

Published online: 27 March 2019

Abstract
The case is made here for the power of using atomic layer deposition (ALD) as a way to induce changes in the nature of the oxides used as supports in many catalytic processes. ALD provides a route to grow thin films in a conformal way and with submonolayer thickness control, affording the creation of unique mixed-oxide structures with new reaction sites. This approach is exemplified here for the case of the hydrogenation of unsaturated aldehydes with platinum-based catalysts. Silica-supported catalysts were modified with thin alumina films, grown by ALD using trimethylaluminum(III) (TMA) and water, and their performance contrasted with pure Pt/SiO_2 and Pt/Al_2O_3 samples as well as with catalysts previously reported by us made by silica ALD on Pt/Al_2O_3. The quality of the alumina films grown on Pt/SiO_2 was first evaluated by using N_2 adsorption–desorption isotherms in conjunction with SBA-15 as the support, a mesoporous material with well-defined 1D cylindrical pores. An initial deposition of approximately 1.5 Å of the alumina film per ALD cycle was estimated from those measurements, with retention of the narrow distribution of pore diameters indicative of homogeneous coverage throughout the length of the pores. The catalytic hydrogenation of cinnamaldehyde was then determined to be slower but more selective with silica supports compared to alumina. Addition of a half of a monolayer of alumina to Pt/SiO_2 reduces the total activity, but only marginally. In exchange, the new mixed-oxide catalysts exhibit a higher selectivity toward the production of the desirable unsaturated alcohol at high conversions, and a lower activity for its subsequent hydrogenation to the saturated alcohol. These trends were associated with the formation of new Brønsted and Lewis acidic sites, possibly based on mixed Si–O–Al surface structures.

Keywords Atomic layer deposition · Unsaturated aldehyde hydrogenation · C=O vs. C=C hydrogenation selectivity · Adsorption–desorption isotherms · Pyridine titrations

1 Introduction

One of the major challenges in heterogeneous catalysis is the design and preparation of highly stable and selective catalysts [1–4]. One versatile way to create new catalytic sites on solids and to tune their properties is by exploiting the unique properties of solid–solid interfaces. Specifically, the area around the contact between two oxides displays electronic and chemical properties that may be quite different to those of the interacting pure phases and that can typically lead to the creation of new acidic sites, different structural atomic ensembles, and/or changes in redox properties [5–9]. Similarly, the interfaces between oxides and metals may provide new mixed sites capable of reacting in unique ways [10–17]. The challenge is to create those interfaces in a controlled way. Many mixed oxides can be made with well-defined compositions and structures, as in the case of zeolites [18, 19], but that still provides limited control on the details of their surfaces, where the catalysis takes place. Procedures that rely on the post-modification of surfaces after the synthesis of the solids afford a more direct route to

Invited contribution to the special issue entitled "6th San Luis Conference on Surfaces, Interfaces and Catalysis.

✉ Francisco Zaera
zaera@ucr.edu

[1] Department of Chemistry and UCR Center for Catalysis, University of California, Riverside, CA 92521, USA

[2] Present Address: Department of Polymer Science & Engineering, Dalian University of Technology, Dalian 116024, People's Republic of China

the design of unique catalytic sites [20–24], yet many traditional treatments such as impregnations and precipitations yield surfaces with ill-defined characteristics. Fortunately, new molecularly designed deposition processes have become available in recent years to improve on the control that can be exerted during the preparation of specific atomic ensembles on surfaces [25–27]. From these, we here focus on the incorporation of atomic layer deposition (ALD) [28–34] to the synthesis of mixed-phase catalysts.

ALD is a chemical approach originally introduced for digital display manufacturing, microelectronics fabrication, and other related applications [35, 36]. In ALD, the deposition chemistry is split into two or more self-limiting and complementary reactions in order to provide a better handle on the thickness, conformality, and uniformity of the grown films [28, 37–41]. ALD is presently considered the deposition method with the greatest potential for the production of thin films with atomic-level precision [36], offering many advantages over other chemical vapor deposition (CVD) processes, at least on flat surfaces [38, 42]: (1) the film thickness depends only on the number of cycles employed, not on the exposures used in each cycle, so process control is simple and accurate; (2) there is less of a need for a homogeneous flux of the reactants through the reactor, a fact that makes processes reproducible and easy to scale for large-area coatings without sacrificing conformality; (3) ALD offers more flexibility in the design of the operational deposition conditions, requiring lower temperatures than regular CVD; (4) there is minimal or no interference from gas-phase reactions during the deposition process because of the separation of the two complementary reactions in time; and (5) it is ease to extend ALD processes to the manufacturing of layered structures. Some of these characteristics of ALD may not be as applicable to porous materials, though, as we have already reported recently [43].

We here address the specific case of making mixed silica-alumina surfaces by ALD to, with the addition of platinum nanoparticles, tune selective hydrogenation catalysis. Both silica and alumina are common supports in catalysis, and specific acidic sites may be added to silica surfaces via the deposition of alumina [8, 18, 19, 44, 45]. Specifically, the substitution of silicon atoms with aluminum in the oxide network provides for a way to add Lewis acid sites, and the change in the electron distribution in adjacent sites also leads to an increase in Brønsted acidity in silanol groups in the vicinity of the Al centers. Hence, the overall acidity of zeolites, for instance, typically depends on the final Al/Si atomic ratio. Similar changes have been pursued and achieved with amorphous silica-alumina solids (ASA), although the new sites sometimes exhibit characteristics different to those seen in zeolites. Also, new structures such as pentacoordinated or distorted tetrahedral Al may be created by alumina addition to those materials [8, 20, 46].

As a guiding principle, we here propose that the acidity of amorphous and mesoporous silica and alumina supports may be modified, and their properties fine-tuned, via the controlled addition of aluminum or silicon oxide layers to their surfaces, respectively, by ALD. This idea is certainly advanced by recent reports where the surfaces of silica and alumina supports have been modified via the deposition of reactive precursors [19, 27, 47, 48]. For instance, silication of γ-alumina with tetraethoxysilane (TEOS) was shown to result in the formation of a surface spinel phase where silicon substitutes for aluminum in tetrahedral sites, exposing surface silanol groups with limited Brønsted acidity, not enough to protonate pyridine at room temperature; this catalyst showed an increase in activity for n-butene isomerization without any loss in selectivity to isobutene [49]. In a separate study with similar samples, "mild" Brønsted acid sites were identified exhibiting identical selectivity but much higher specific activity than the parent alumina for the liquid-phase catalytic dehydration of cyclohexanol [26]. In yet another investigation, deposition of trimethylaluminum (TMA) on faujasite-type catalysts led, after proper conditioning, to higher propane cracking activity per Brønsted acid site [22]. Deposition of aluminum species on hydroxylated silica has also been shown to create new sites active for ethanol dehydration and m-xylene isomerization [50]. Some spectroscopic studies have been directed at identifying the new sites made by these surface modifications of silica and alumina amorphous solids, but their structure is still a matter of debate [25]: the original models that Brønsted acidity arises from protons compensating the electronic charge of the surface or from Al–OH groups close to silanol groups [51–53] have been challenged by new ideas that include acidic sites similar to those of zeolites, that is, bridging Si–OH–Al groups [54–56], and silanol groups in the vicinity of aluminum atoms but not bridging to OH moieties with aluminum atoms in different coordination spheres, including tetrahedral Al(IV), five-coordinate Al(V), and unsaturated Al(III) [57, 58].

Here we report on the modification of Pt catalysts based on silica porous materials with alumina thin films. The modification of pure silica (without any dispersed metal nanoparticles) via the addition of alumina films has already been reported in the past in a few selected cases [59, 60]. Typically, alumina can be deposited by alternating trimethylaluminum (TMA) and water in ALD cycles under mild conditions, that is, at temperatures on the order of 200 °C or less. This chemistry has been quite well characterized on flat surfaces [61, 62], and also demonstrated in porous materials such as zeolites [29, 60, 63–66] and other supported catalysts [67, 68]. We have in fact already successfully tested the growth of alumina films on the walls of the pores of pure SBA-15 using this type of ALD with TMA and water, as we reported recently [43]. We found that each ALD cycle leads to a reduction in average pore diameter

of about 0.3 nm while still retaining most of the narrow distribution of pore sizes present in the original material. In this work we have applied the same approach to modify Pt/SiO_2 catalysts, with the idea of adding new acidic sites to control selectivity during the hydrogenation of unsaturated organic reactants, specifically of unsaturated aldehydes.

Past studies on the selective hydrogenation of C=O bonds over C=C bonds in such aldehydes have concluded that both acidic and redox functionality affect the performance of the dispersed transition metal phase [69–72]. It has also been reported that the use of reducible supports such as TiO_2 increases selectivity towards unsaturated alcohols [73, 74], presumably because of a strong metal-support interaction (SMSI) effect exerted by the new oxide on the metal phase. In a previous publication we described the effects of adding silica films to Pt/Al_2O_3 catalysts [75], the reverse of the case studied here. It was found that the silica layers greatly increase the stability of the platinum nanoparticles, preventing their sintering during high-temperature calcinations without affecting access to the metal surface in any significant way. It was also established that Pt/Al_2O_3 promotes this hydrogenation at more than twice the rate seen with Pt/SiO_2 but with much lower selectivity toward the production of the unsaturated alcohol, typically the desired product. Additional Brønsted and Lewis acid sites were created upon the deposition of submonolayer coverages of silicon oxide, as probed via pyridine adsorption. The addition of the silicon oxide thin films reduced the overall activity of these catalysts but also increased their selectivity toward the production of the unsaturated alcohol. The best catalysts in term of selectivity were obtained after 3 or 4 SiO_2 ALD cycles, which were estimated to deposit approximately half of a monolayer (~ 1 Å) of SiO_2 [43]. Based on these results, it was proposed that the added strong Brønsted acid sites at mixed Si–O–Al positions, possibly in synergy with the metal surface, may be responsible for the relative enhancement in the hydrogenation of C=O bonds detected. In the experiments described below, we explore this possibility further by approaching the preparation of the Pt-based silica-alumina mixed-oxide catalysts from the other end, starting with silica supports and adding controlled amounts of alumina on top. Improvements in catalytic performance were seen with the new catalysts, as described below, and synergies were identified, as before, that lead to changes in both activity and selectivity that cannot be simply explained by a linear combination of the performance of the two oxide phases.

2 Experimental Details

Two Pt/silica catalysts were used for these studies: (1) a commercial 1 wt% Pt/SiO_2 solid, purchased from Sigma-Aldrich, which was employed to test the catalytic conversion of cinnamaldehyde; and (2) 3 wt% Pt/SBA-15, made in house (by mixing a H_2PtCl_6 solution with SBA-15, evaporating the solvent under vacuum at 310 K, calcining the resulting solid in air at 675 K for 2 h, and reducing the metal under H_2 at 625 K for 2 h prior to use) and used for the adsorption–desorption isotherm measurements and the infrared spectroscopy characterization of pyridine adsorption. The SBA-15 was purchased from Sigma-Aldrich SBA-15 ($\geq$ 99.9% SiO_2 purity, surface area = 700 ± 50 $m^2\ g^{-1}$, pore volume = 0.5–0.7 $cm^3\ g^{-1}$, pore diameter > 6 nm, particle size < 150 μm).

The Al_2O_3 ALD film growth was carried out in a homemade reactor based on a six-way stainless steel cross by following a procedure described in detail elsewhere [43], alternating doses of trimethylaluminum(III) (TMA) and deionized water at 475 K with Ar flushings in between. The powder was thinly spread on the Ni-based tray of the reactor to assure even exposure to the reactants (also discussed extensively previously [43]). The additional data reported for Pt/Al_2O_3 catalysts, by itself and after SiO_2 ALD film growth, are from a previous study in our laboratory [75].

N_2 adsorption–desorption isotherms were carried out using a NOVA@2000e gas sorption system. The adsorption of pyridine was characterized by infrared absorption spectroscopy in transmission mode, using a homemade quartz cell with NaCl windows and a Bruker Tensor 27 Fourier-transform infrared (FTIR) spectrometer [75–77]. The kinetic measurements were performed using a 300 mL high-pressure Parr batch reactor [72, 75]. Aliquots of the reaction mixture were taken periodically (every half an hour at the beginning, more infrequently later on) and analyzed by gas chromatography. Turnover numbers were estimated by using the total Pt loading of the catalysts, and expressed in terms of molecules converted per Pt atom. Given that only about half of the Pt atoms in these catalysts may be exposed at the surface of the nanoparticles (NPs) [75], our reported TON values systematically underestimate the real extent of conversion, but relative comparisons are not affected by this factor. Turnover frequencies (TOFs) were then calculated via numerical derivatization of the TON versus time data, and expressed in TON/h.

3 Results and Discussion

The effectiveness of the Al_2O_3 ALD procedure to grow uniform films on the Pt/silica catalysts was evaluated via analysis of data from N_2 adsorption–desorption isotherm experiments performed on Pt/SBA-15 samples. As discussed in detail in a previous publication, the uniform pore size and shape of the pores in mesoporous materials such as SBA-15 can be exploited to evaluate the characteristics of the thin films grown by ALD: the pore size distributions can provide

information about deposition rates and the uniformity of the films, whereas the changes in pore surface area and pore volume can be used to independently assess the extent of the deposition [43]. Typical data recorded in the experiments reported here for (Al_2O_3 ALD)/Pt/SBA-15 samples are presented in Fig. 1.

The left panel of Fig. 1 displays the uptake and desorption of N_2 as a function of pressure for four samples, the original catalyst as well as (Al_2O_3 ALD)/Pt/SBA-15 samples obtained after 1, 3, and 5 ALD cycles. The results (the adsorption isotherms as well as the pore size distributions) are very similar to those reported previously with (Al_2O_3 ALD)/SBA-15 samples, without any added Pt [43], a comparison that indicates that the dispersed Pt NPs do not appear to affect the ALD process. The following observations are worth highlighting: (1) the normalized total pore volume (that is, the N_2 volume absorbed at $P/P_0 = 1$ per gram of catalyst), decreases with increasing number of ALD cycles, because of the empty space in the pores taken by the growing new film [43]; and (2) the shape of the hysteresis loop between the adsorption and desorption branches is not affected by the film deposition, indicating retention of the original cylindrical geometry of the pores.

The right panel of Fig. 1 reports the pore size distributions calculated from the data for the N_2 desorption process in the left panel using the BJH (Barrett–Joyner–Halenda)

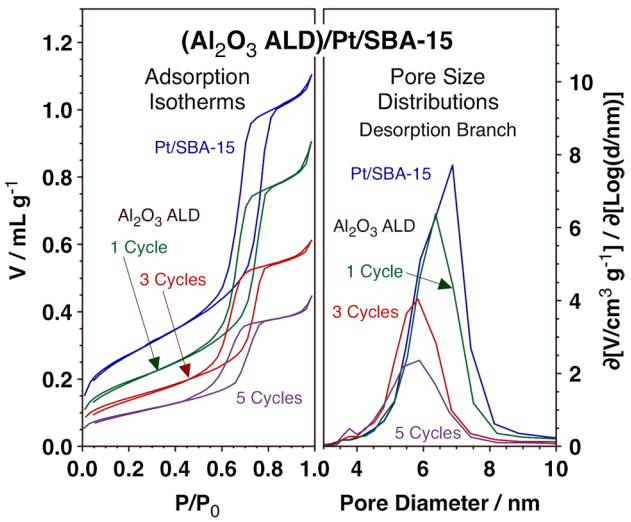

Fig. 1 Left: N_2 adsorption–desorption isotherms, in the form of uptake volume versus pressure, for Pt/SBA-15 samples on which aluminum oxide thin films have been deposited by ALD. Data are reported as a function of the number of ALD cycles (0, 1, 3, and 5) used. Right: Pore size distributions extracted from analysis of the desorption branch of the curves reported in the left panel. The monotonic pore size decrease seen with increasing number of ALD cycles, together with the preservation of the narrow size distribution, reflects the uniform nature of the deposition process and the growth of a film by about 1.5 Å in thickness per cycle in the initial stages of the deposition

equation for Type IV isotherms [78]. It is clear that the pore size decreases monotonically with increasing number of ALD cycles. More importantly, the size distributions retain their narrow nature, attesting to the good quality (uniformity) of the newly grown Al_2O_3 films. An initial deposition of films 1.5 ± 0.2 Å in thickness per ALD cycle was calculated from this data, virtually the same (within experimental error) to that seen with the SBA-15 samples without Pt [43], and also consistent with typical alumina ALD growth on other substrates [61, 79, 80]. Access of the reactants in catalysis to the surface of the Pt nanoparticles is preserved in these catalysts even after the deposition of the alumina films, a fact shown previously by using carbon-monoxide titration experiments with infrared absorption spectroscopy [75]. On the other hand, partial blocking of metal sites by the grown films is possible, as discussed below.

The catalytic performance of the solids prepared by alumina ALD on commercial Pt/SiO_2 for the promotion of hydrogenation reactions was tested next. Specifically, these catalysts were evaluated for the selective hydrogenation of conjugated unsaturated aldehydes (cinnamaldehyde in particular). The reactions considered here are depicted in Scheme 1. Typically, there is an interest in selectively promoting the hydrogenation of the aldehyde group of unsaturated aldehydes to yield unsaturated alcohols, the conversion of cinnamaldehyde (CMA) to cinnamyl alcohol (CMO) in our particular case, because the resulting products are valuable feedstocks for the making of flavorings, perfumes, and pharmaceuticals [69, 70, 81, 82]. In general, however, reported selectivities to the desirable allyl alcohol production are low, especially when using Pt-based catalysts, which tend to favor C=C double bond hydrogenation to dihydrocinnamaldehyde (HCMA) instead, or even full hydrogenation to dihydrocinnamyl alcohol (HCMO) [70–72, 83–86]. In this work we explore the possibility of tuning such selectivity by modifying the properties of the support in a controlled manner, via ALD.

Typical kinetic data in the form of turnover numbers (TONs) versus time resulting from these studies are reported in Fig. 2. Results are shown for the total CMA conversion as well as for the accumulation of all three individual products in the reaction mixture under the following conditions: cinnamaldehyde/Pt mole ratio = 500:1, $P(H_2) = 30$ bar, $T = 300$ K. Kinetics for four samples are reported: for Pt/SiO_2 as is and after 5 Al_2O_3 ALD cycles, measured in this study, and for Pt/Al_2O_3 naked and after 4 SiO_2 ALD cycles, from our previous work [75]. The number of ALD cycles used in both cases was chosen to correspond to approximately half a monolayer of coverage of the new oxide film, to produce the mixed silica-alumina surfaces that showed the most promise before [75]. We'll return to this point later.

Figure 2 clearly shows that the highest activity, both total and partial for each of the products, is obtained with

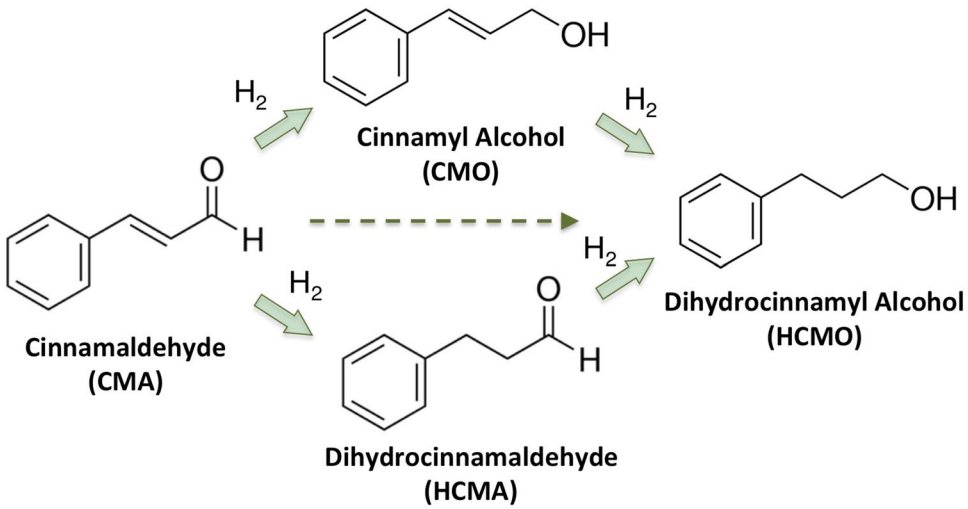

Scheme 1 Reaction network considered here for the hydrogenation of cinnamaldehyde (CMA). Particular focus is placed on the selective production of cinnamyl alcohol (CMO) over dihydrocinnamaldehyde (HCMA)

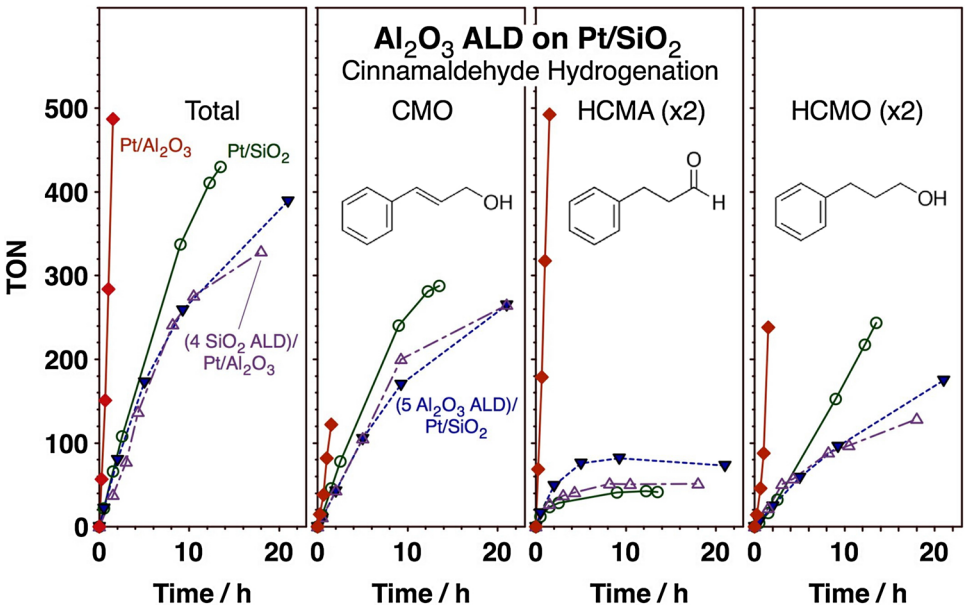

Fig. 2 TONs versus time for the hydrogenation of cinnamaldehyde (CMA) on Pt/SiO_2 and Pt/Al_2O_3 catalysts, unmodified and after ALD of approximately half a monolayer of aluminum oxide or silicon oxide, respectively. Shown are the data for the total conversion (left panel) as well as for the production of CMO (second panel), HCMA (third panel), and HCMO (last panel). The alumina-based catalyst is more active but less selective, whereas the mixed-oxide supported samples show subtle but desirable changes compared to the Pt/SiO_2 case

the pure alumina support, a result consistent with past publications [70, 87, 88]. By contrast, the rate of conversion is much slower, as much as one order of magnitude lower, on silica-based catalysts. In terms of the ALD-treated catalysts, the two cases reported here, namely, the (5 Al_2O_3 ALD)/Pt/SiO_2 and (4 SiO_2 ALD)/Pt/Al_2O_3 samples, display similar performance, suggesting that their surfaces may be similar. As already mentioned before, we argue that the number of ALD cycles chosen in both cases leads to the deposition of approximately half a monolayer of the new oxide, and results in the likely formation of new Si–O–Al surface sites. The total conversion rates with those catalysts is marginally lower than with Pt/SiO_2, suggesting that perhaps the Pt NPs may become slightly covered by the ALD films, reducing the active catalytic areas.

The data in Fig. 2 also show a slowing down in conversion with reaction time, with trends that differ for the different individual products. This is likely to be indicative of changes that may take place on the surface of the catalyst under reaction conditions, although it may alternatively reflect the effect of the presence of the products in the reaction mixture, as these reactions were performed in a batch reactor. In order to better follow the changes in conversion over time, the raw kinetic data was converted into TOFs (Fig. 3), and the new numbers used to estimate reaction selectivities (Fig. 4). Figure 3 shows how the total rate of conversion with both the original Pt/SiO_2 catalyst and with the sample obtained after 4 Al_2O_3 ALD cycles decreases with reaction time. The approximately linear way in which that happens indicates a first-order dependence of

the reaction rate on the concentration of the reactant (CMA) in the solution, a behavior easy to understand if the process involves individual adsorbed reactants at low coverages on the surface. However, the trends seen with the individual products suggest a more nuanced overall kinetic scheme. Indeed, one significant observation in Fig. 3 is the fact that the rate of CMO production increases with reaction time in the early stages of the conversion, apparently at the expense of the HCMA production. This trend, which we have also seen with alumina-based samples [75], strongly suggests that the catalysts need to be conditioned under the highly reducing conditions of the reaction before reaching a steady-state behavior. After a couple of hours, though, the initial rate increase reverses itself, and both the total activity and those for the production of both CMO and HCMA go down over time afterwards. The TOF for HCMO production does not seem to change significantly over time, reflecting zero-order dependences on the concentration of the reactant (CMA) and the products (CMO and HCMA).

The traces in the two panels of Fig. 3 do in general show similar behavior with the two catalysts considered, Pt/SiO_2 without versus with an added Al_2O_3 ALD layer: both the total TOFs and the trends versus reaction time are comparable. There are, however, some subtle but significant differences that are better highlighted in the plots of selectivities versus time (left panel) and conversion (right panel) provided in Fig. 4. As mentioned before,

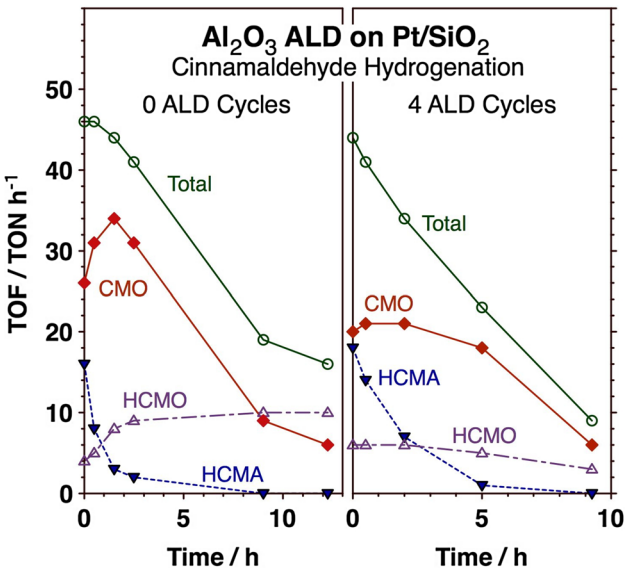

Fig. 3 TOFs versus reaction time for the hydrogenation of cinnamaldehyde promoted by Pt/SiO_2 catalysts, unmodified (left panel) and after being covered with a thin alumina film (deposited using 4 ALD cycles, right panel). Data are shown for the total conversion as well as for each individual product, calculated by numerical differentiation of the original results shown in Fig. 2. Interestingly, the TOFs for CMO initially increase with reaction time at the expense of HCMA production

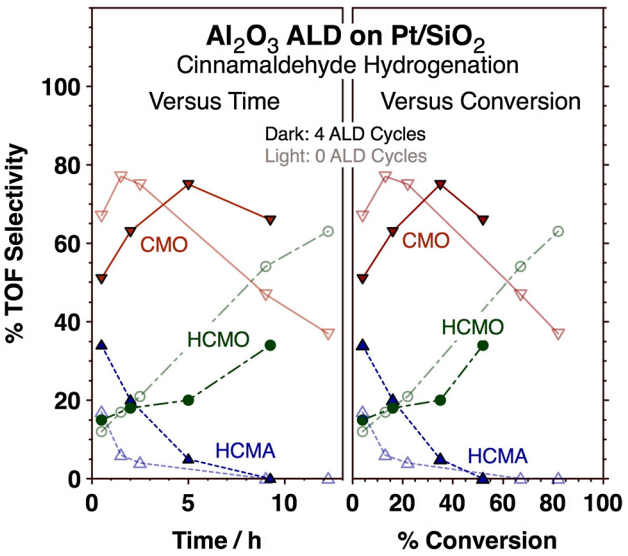

Fig. 4 Selectivities, calculated in terms of TOFs, for CMO, HCMO, and HCMA. The data are displayed in terms of both reaction time (left panel) and the extent of conversion (right). Two sets of data are provided, for Pt/SiO_2 (light traces, open symbols) and for (4 Al_2O_3 ALD)/Pt/SiO_2 (dark lines, filled symbols). The maximum in CMO selectivity is reached at later times and at higher conversions with the ALD-modified catalysts, which then retains better selectivity at high conversions

the selectivity for CMO production goes up in the early stages of the reaction, but reverses after a few hours. The selectivity toward HCMA production decreases monotonically with increasing reaction time or conversion, however, which means that the changes in the kinetics of CMO are due primarily the consumption of the reactant (CMA) and the subsequent conversion of CMO to HCMO. It is also important to note that the net TOF for HCMA reaches values close to zero in the later stages of the CMA conversion but do not become negative, indicating that it is much more difficult to further hydrogenate HCMA than CMO to HCMO within these reaction mixtures.

In terms of the comparative behavior of Pt/SiO_2 versus (4 Al_2O_3 ALD)/Pt/SiO_2, Fig. 4 clearly shows that, because the ALD-treated sample takes longer to fully condition at the start of the reaction, it takes longer to reach the maximum in CMO selectivity, but also, as a consequence, retains a higher CMO selectivity afterwards; further hydrogenation of CMO to HCMO is delayed. In fact, the rate for HCMO production is always lower with the modified catalyst (Fig. 3), which means that the added alumina film also induces an intrinsic change in selectivity. This is a desirable change, as it implies that a flow-reactor process with good CMO selectivity could be setup with the mixed-oxide catalysts at higher conversions than possible with pure silica supports. Notice that, after approximately 10 h of reaction, both the Pt/SiO_2 and (4 Al_2O_3 ALD)/Pt/SiO_2 catalysts show similar

CMO TOFs, but that the silica-only catalyst shows higher HCMO TOF (Fig. 3).

In search for an explanation for the higher ultimate selectivity achieved by the mixed-oxide catalysts at the later stages of the conversion, in particular the suppression of the hydrogenation of CMO to HCMO, pyridine-infrared spectroscopy (IR) titration studies were performed to identify new possible acidic sites [89–91]. The data obtained from this work are summarized in Fig. 5. There, IR traces are shown for (x Al_2O_3 ALD)/Pt/SBA-15 (x = 0, 3, 5) and (y SiO_2 ALD)/Pt/Al_2O_3 (x = 0, 6) after surface saturation with pyridine at 300 K (left panel) and after annealing to 425 K to desorb any weakly adsorbed species (right panel). Most of the peaks observed here are expected, and have been reported and assigned before. Specifically, the two main features at 1447 and 1595 cm^{-1} are associated with hydrogen-bonded pyridine, and the additional bands at 1492, 1578, and 1614 cm^{-1} originate from coordinately bonded pyridine on Lewis acidic sites [92, 93]. All those peaks are clearly seen with all the samples at low (300 K) temperatures, because pyridine can bind weakly and show similar behavior on both silica and alumina supports under those conditions.

The data recorded after annealing at 425 K is more discriminating, however, as those only shows relatively strongly bonded species. For one, there are clear differences in peak intensities between the samples based on silica versus alumina supports, with the spectra from the former mainly showing hydrogen-bonded pyridine and the data for the latter also displaying features for adsorption on Lewis acid sites (the hydrogen-bonded pyridine features are weaker in those cases). The spectra from the samples modified by ALD display most of the features of the alumina-only catalyst, but also show some subtle differences indicative of a synergy between the silicon oxide and the aluminum oxide. In particular, the peak at 1492 cm^{-1} seems to be the most intense for the (3 Al_2O_3 ALD)/Pt/SBA-15 sample, and to show much less intensity in samples with higher alumina content. Perhaps more interestingly, new features develop at 1547 and 1620 cm^{-1}, the latter seen as a shoulder of the 1614 cm^{-1} feature in the traces for the (3 Al_2O_3 ALD)/Pt/SBA-15 and (6 SiO_2 ALD)/Pt/Al_2O_3 and more clearly in the data for (5 Al_2O_3 ALD)/Pt/SBA-15. The first is typically associated with pyridinium ions, and is indicative of adsorption on strong Brønsted acid sites, whereas the latter has been ascribed to strong Lewis sites [94]. These new acidic sites are likely to be responsible for the changes in selectivity during the hydrogenation of cinnamaldehyde seen with Pt/SiO_2 catalysts upon the addition of thin alumina layers.

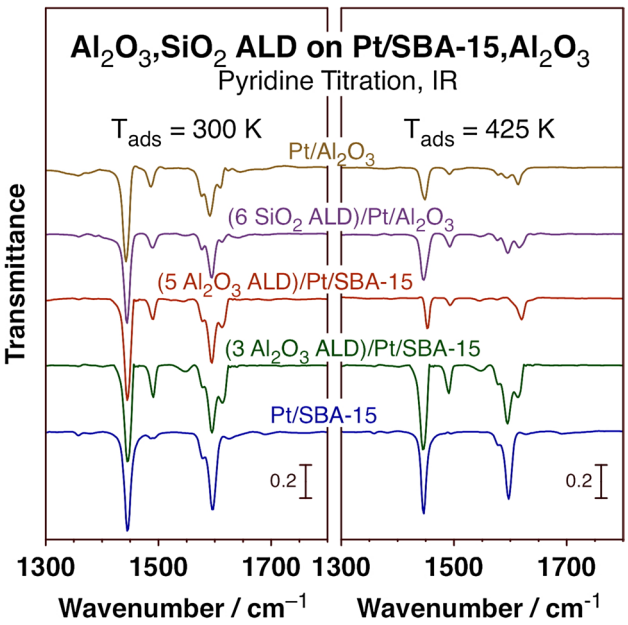

Fig. 5 IR absorption spectra of pyridine adsorbed at 300 K (left panel) and 425 K (right panel) on Pt/SiO_2 and Pt/Al_2O_3 catalysts, unmodified and after ALD of thin alumina or silicon oxide films of different thicknesses, respectively (after 3 and 5 Al_2O_3 ALD cycles on the silica substrate and after 6 SiO_2 ALD on the alumina based sample). The new peaks that develop at 1547 and 1620 cm^{-1} in the ALD-modified catalysts indicate the creation of new strong Brønsted and Lewis sites, respectively, on the mixed oxide surfaces

4 Conclusions

A brief discussion has been provided in the Introduction of this report on the merits of using atomic layer deposition (ALD) as a way to prepare new catalysts in a controlled way to improve on catalytic performance. ALD affords the deposition of thin films of metal oxides on porous materials in an even and conformal fashion and with submonolayer thickness control, a way to create new mixed-oxide sites on the surface of catalysts. This ALD approach to catalyst design was illustrated here for the modification of Pt-based catalysts used for the selective hydrogenation of unsaturated aldehydes, cinnamaldehyde in our example. Silica supported catalysts were modified via the addition of thin alumina films, and their performance contrasted to alumina based catalysts modified by silica ALD, which we had studied before and reported in a previous publication [75]. First, the quality of the alumina films was assessed by recording N_2 adsorption–desorption isotherms, using SBA-15 as the silica support to take advantage of the well defined geometry of the pores in that material. It was shown that the average pore diameter is reduced monotonically with increasing alumina ALD cycles, as expected because of the blockage induced by the new grown films; an initial deposition rate of about 1.5 Å/ALD cycle was estimated from these results. Significantly, the narrow nature of the pore diameter distribution of SBA-15 was retained upon the ALD addition of alumina films, indicating that the deposition is homogeneous all throughout

the surfaces of the pores. Decreases in total pore volume and surface area were seen as well, consistent with the picture of an even coating of the mesopores by the new alumina films. The behavior seen here during Al_2O_3 ALD on Pt/SBA-15 matches quite closely that reported by us in the past for pure SBA-15 samples, without Pt [43], demonstrating that the dispersed Pt nanoparticles do not affect the ALD process in any significant way.

The ALD-modified catalysts were tested for the hydrogenation of cinnamaldehyde. As reported before [75], we found that alumina-based catalysts are much more active but less selective for this reaction than those made out of Pt nanoparticles dispersed on silica. Catalysts made by addition of alumina thin films to Pt/SiO_2 showed performances comparable to the unmodified original material, but a few subtle differences were nevertheless identified. First, a slight decrease in total activity was seen, presumably because of partial site blockage of the metal phase by the deposited alumina films. This drop in activity was small, however, and detectable mostly at high conversion; the initial TOFs were identical with versus without the added alumina films (within experimental error). Perhaps more significant are the changes seen in the selectivity of the hydrogenation catalysis as a function of reaction time. Two observations stand out in this context. First, the selectivity toward the production of the desirable cinnamyl alcohol (CMO) increased with reaction time with all our catalysts in the initial stages of the conversion, at the expense of dihydrocinnamaldehyde (HCMA) formation. This trend, which implies the need for conditioning of the surface under reaction conditions, reverses after a few hours, after which the rate of CMO production decreased linearly with reaction time or conversion, reflecting the expected first-order kinetics. Critically, the transition from increasing to decreasing CMO selectivity was slower with the alumina-modified catalysts, which means that maximum selectivity is reached at higher conversions with those. This is a desirable outcome, as it suggests that the mixed-oxide catalysts should be better in terms of selectivity for operation in flow reactors under high conversion conditions.

The second important observation in these kinetic studies was that dihydrocinnamyl alcohol (HCMO) production is partially suppressed by the added alumina films. HCMO is mainly made as a secondary product, via further hydrogenation of the primary CMO and HCMA products (although in some circumstances it can be produced directly on the surface of the metal catalyst in a concerted way [95]), but in our mixed-oxide systems it seems to come from hydrogenation of CMO only. Accordingly, the suppression of this secondary step seen with the ALD-modified catalysts is also desirable, as it helps increase selectivity toward CMO. The suppression of the extensive hydrogenation of cinnamaldehyde (CMA) to HCMO correlates with the creation of new Brønsted and Lewis sites on the mixed-oxide surfaces, as identified by the new peaks seen at 1547 and 1620 cm^{-1} in the IR spectra of pyridine adsorbed on these catalysts, respectively. Since the coverages of the oxides added by ALD that lead to optimum catalytic performance amount to approximately half a monolayer, we speculate that the new chemistry may be associated with new Si–O–Al surface sites.

Acknowledgements Financial support for this project was provided by a Grant from the U.S. National Science Foundation, Division of Chemistry, under Award No. NSF-1660433.

References

1. Hutchings GJ (2005) Commentary on industrial processes. Philos Trans R Soc B 363(1829):985–987. https://doi.org/10.1098/rsta.2004.1531
2. Smit B, Maesen TLM (2008) Towards a molecular understanding of shape selectivity. Nature 451(7179):671–678. https://doi.org/10.1038/nature06552
3. Somorjai GA, Park JY (2008) Molecular factors of catalytic selectivity. Angew Chem Int Ed 47(48):9212–9228. https://doi.org/10.1002/anie.200803181
4. Zaera F (2010) The new materials science of catalysis: toward controlling selectivity by designing the structure of the active site. J Phys Chem Lett 1(3):621–627. https://doi.org/10.1021/jz9002586
5. Corma A, García H (2003) Lewis acids: from conventional homogeneous to green homogeneous and heterogeneous catalysis. Chem Rev 103(11):4307–4366. https://doi.org/10.1021/cr030680z
6. Wachs IE (2005) Recent conceptual advances in the catalysis science of mixed metal oxide catalytic materials. Catal Today 100(1–2):79–94. https://doi.org/10.1016/j.cattod.2004.12.019
7. Frenzer G, Maier WF (2006) Amorphous porous mixed oxides: sol-gel ways to a highly versatile class of materials and catalysts. Annu Rev Mater Res 36:281–331. https://doi.org/10.1146/annurev.matsci.36.032905.092408
8. Busca G (2007) Acid catalysts in industrial hydrocarbon chemistry. Chem Rev 107(11):5366–5410. https://doi.org/10.1021/cr068042e
9. Debecker DP, Hulea V, Mutin PH (2013) Mesoporous mixed oxide catalysts via non-hydrolytic sol–gel: a review. Appl Catal A 451:192–206. https://doi.org/10.1016/j.apcata.2012.11.002
10. Diebold U, Pan J-M, Madey TE (1995) Ultrathin metal film growth on TiO_2(110): an overview. Surf Sci 331:845–854. https://doi.org/10.1016/0039-6028(95)00124-7
11. Hammer B (2006) Special sites at noble and late transition metal catalysts. Top Catal 37(1):3–16. https://doi.org/10.1007/s11244-006-0004-y
12. Haruta M (2011) Spiers memorial lecture role of perimeter interfaces in catalysis by gold nanoparticles. Faraday Discuss 152:11–32. https://doi.org/10.1039/C1FD00107H
13. de la Peña O'Shea VA, Álvarez Galván MC, Platero Prats AE, Campos-Martin JM, Fierro JLG (2011) Direct evidence of the SMSI decoration effect: the case of Co/TiO_2 catalyst. Chem Commun 47(25):7131–7133. https://doi.org/10.1039/c1cc10318k
14. Wu B, Zheng N (2013) Surface and interface control of noble metal nanocrystals for catalytic and electrocatalytic applications. Nano Today 8(2):168–197. https://doi.org/10.1016/j.nantod.2013.02.006
15. Mudiyanselage K, Senanayake SD, Feria L, Kundu S, Baber AE, Graciani J, Vidal AB, Agnoli S, Evans J, Chang R, Axnanda S,

Liu Z, Sanz JF, Liu P, Rodriguez JA, Stacchiola DJ (2013) Importance of the metal–oxide interface in catalysis: in situ studies of the water–gas shift reaction by ambient-pressure X-Ray photoelectron spectroscopy. Angew Chem Int Ed 52(19):5101–5105. https://doi.org/10.1002/anie.201210077
16. An K, Alayoglu S, Musselwhite N, Plamthottam S, Melaet G, Lindeman AE, Somorjai GA (2013) Enhanced CO oxidation rates at the interface of mesoporous oxides and Pt nanoparticles. J Am Chem Soc 135(44):16689–16696. https://doi.org/10.1021/ja4088743
17. Liu XY, Wang A, Zhang T, Mou C-Y (2013) Catalysis by gold: new insights into the support effect. Nano Today 8(4):403–416. https://doi.org/10.1016/j.nantod.2013.07.005
18. Martínez C, Corma A (2011) Inorganic molecular sieves: preparation, modification and industrial application in catalytic processes. Coord Chem Rev 255(13/14):1558–1580. https://doi.org/10.1016/j.ccr.2011.03.014
19. Caillot M, Chaumonnot A, Digne M, van Bokhoven JA (2014) The variety of Brønsted acid sites in amorphous aluminosilicates and zeolites. J Catal 316:47–56. https://doi.org/10.1016/j.jcat.2014.05.002
20. Hensen EJM, Poduval DG, Magusin PCMM, Coumans AE, van Veen JAR (2010) Formation of acid sites in amorphous silica-alumina. J Catal 269(1):201–218. https://doi.org/10.1016/j.jcat.2009.11.008
21. Ungureanu A, Dragoi B, Hulea V, Cacciaguerra T, Meloni D, Solinas V, Dumitriu E (2012) Effect of aluminium incorporation by the "pH-adjusting" method on the structural, acidic and catalytic properties of mesoporous SBA-15. Microporous Mesoporous Mater 163:51–64. https://doi.org/10.1016/j.micromeso.2012.05.007
22. Pidko EA, Almutairi SMT, Mezari B, Magusin PCMM, Hensen EJM (2013) Chemical vapor deposition of trimethylaluminum on dealuminated faujasite zeolite. ACS Catal 3(7):1504–1517. https://doi.org/10.1021/cs400181p
23. González MD, Salagre P, Mokaya R, Cesteros Y (2014) Tuning the acidic and textural properties of ordered mesoporous silicas for their application as catalysts in the etherification of glycerol with isobutene. Catal Today 227:171–178. https://doi.org/10.1016/j.cattod.2013.10.029
24. Mardkhe MK, Huang B, Bartholomew CH, Alam TM, Woodfield BF (2016) Synthesis and characterization of silica doped alumina catalyst support with superior thermal stability and unique pore properties. J Porous Mater 23(2):475–487. https://doi.org/10.1007/s10934-015-0101-z
25. Valla M, Rossini AJ, Caillot M, Chizallet C, Raybaud P, Digne M, Chaumonnot A, Lesage A, Emsley L, van Bokhoven JA, Copéret C (2015) Atomic description of the interface between silica and alumina in aluminosilicates through dynamic nuclear polarization surface-enhanced NMR spectroscopy and first-principles calculations. J Am Chem Soc 137(33):10710–10719. https://doi.org/10.1021/jacs.5b06134
26. Mouat AR, George C, Kobayashi T, Pruski M, van Duyne RP, Marks TJ, Stair PC (2015) Highly dispersed SiO_x/Al_2O_3 catalysts illuminate the reactivity of isolated silanol sites. Angew Chem Int Ed 54(45):13346–13351. https://doi.org/10.1002/anie.201505452
27. Ardagh MA, Bo Z, Nauert SL, Notestein JM (2016) Depositing SiO_2 on Al_2O_3: a route to tunable Brønsted acid catalysts. ACS Catal 6(9):6156–6164. https://doi.org/10.1021/acscatal.6b01077
28. George SM (2010) Atomic layer deposition: an overview. Chem Rev 110(1):111–131. https://doi.org/10.1021/cr900056b
29. Detavernier C, Dendooven J, Pulinthanathu Sree S, Ludwig KF, Martens JA (2011) Tailoring nanoporous materials by atomic layer deposition. Chem Soc Rev 40(11):5242–5253
30. Elam JW, Dasgupta NP, Prinz FB (2011) ALD for clean energy conversion, utilization, and storage. MRS Bull 36(11):899–906
31. Zaera F (2013) Nanostructured materials for applications in heterogeneous catalysis. Chem Soc Rev 42(7):2746–2762. https://doi.org/10.1039/c2cs35261c
32. Lu J, Elam JW, Stair PC (2016) Atomic layer deposition—sequential self-limiting surface reactions for advanced catalyst "bottom-up" synthesis. Surf Sci Rep 71(2):410–472. https://doi.org/10.1016/j.surfrep.2016.03.003
33. Singh JA, Yang N, Bent SF (2017) Nanoengineering heterogeneous catalysts by atomic layer deposition. Annu Rev Chem Biomol Eng 8(1):41–62. https://doi.org/10.1146/annurev-chembioeng-060816-101547
34. Meng X, Wang X, Geng D, Ozgit-Akgun C, Schneider N, Elam JW (2017) Atomic layer deposition for nanomaterial synthesis and functionalization in energy technology. Mater Horiz 4(2):133–154. https://doi.org/10.1039/C6MH00521G
35. Schumacher M, Baumann PK, Seidel T (2006) AVD and ALD as two complementary technology solutions for next generation dielectric and conductive thin-film processing. Chem Vap Depos 12(2–3):99–108. https://doi.org/10.1002/cvde.200500027
36. Levitin G, Hess DW (2011) Surface reactions in microelectronics process technology. Annu Rev Chem Biomol Eng 2(1):299–324. https://doi.org/10.1146/annurev-chembioeng-061010-114249
37. Lim BS, Rahtu A, Gordon RG (2003) Atomic layer deposition of transition metals. Nat Mater 2(11):749–754. https://doi.org/10.1038/nmat1000
38. Kim H (2003) Atomic layer deposition of metal and nitride thin films: current research efforts and applications for semiconductor device processing. J Vac Sci Technol, B 21(6):2231–2261. https://doi.org/10.1116/1.1622676
39. Ritala M (2004) Atomic layer deposition. In: Houssa M (ed) High-k Gate Dielectrics. Series in Materials Science and Engineering. Institute of Physics, Bristol; Philadelphia, pp 17–64
40. Zaera F (2012) The surface chemistry of atomic layer depositions of solid thin films. J Phys Chem Lett 3(10):1301–1309. https://doi.org/10.1021/jz300125f
41. Zaera F (2013) Mechanisms of surface reactions in thin solid film chemical deposition processes. Coord Chem Rev 257(23–24):3177–3191. https://doi.org/10.1016/j.ccr.2013.04.006
42. Leskelä M, Ritala M (2003) Atomic layer deposition chemistry: recent developments and future challenges. Angew Chem Int Ed 42(45):5548–5554. https://doi.org/10.1002/anie.200301652
43. Weng Z, Z-h Chen, Qin X, Zaera F (2018) Sub-monolayer control of the growth of oxide films on mesoporous materials. J Mater Chem A 6(36):17548–17558. https://doi.org/10.1039/C8TA05431B
44. Vjunov A, Fulton JL, Huthwelker T, Pin S, Mei D, Schenter GK, Govind N, Camaioni DM, Hu JZ, Lercher JA (2014) Quantitatively probing the Al distribution in zeolites. J Am Chem Soc 136(23):8296–8306. https://doi.org/10.1021/ja501361v
45. Armor JN (2011) A history of industrial catalysis. Catal Today 163(1):3–9. https://doi.org/10.1016/j.cattod.2009.11.019
46. Leydier F, Chizallet C, Chaumonnot A, Digne M, Soyer E, Quoineaud A-A, Costa D, Raybaud P (2011) Brønsted acidity of amorphous silica–alumina: the molecular rules of proton transfer. J Catal 284(2):215–229. https://doi.org/10.1016/j.jcat.2011.08.015
47. Caillot M, Chaumonnot A, Digne M, Bokhoven JAV (2013) Quantification of Brønsted acid sites of grafted amorphous silica-alumina compounds and their turnover frequency in m-xylene isomerization. ChemCatChem 5(12):3644–3656. https://doi.org/10.1002/cctc.201300560
48. Caillot M, Chaumonnot A, Digne M, Poleunis C, Debecker DP, van Bokhoven JA (2014) Synthesis of amorphous aluminosilicates by grafting: tuning the building and final structure of the deposit by selecting the appropriate synthesis conditions. Microporous

Mesoporous Mater 185:179–189. https://doi.org/10.1016/j.micromeso.2013.10.032
49. Finocchio E, Busca G, Rossini S, Cornaro U, Piccoli V, Miglio R (1997) FT-IR characterization of silicated aluminas, active olefin skeletal isomerization catalysts. Catal Today 33(1):335–352. https://doi.org/10.1016/S0920-5861(96)00106-X
50. Caillot M, Chaumonnot A, Digne M, Van Bokhoven JA (2014) Creation of Brønsted acidity by grafting aluminum isopropoxide on silica under controlled conditions: determination of the number of Brønsted Sites and their turnover frequency for m-xylene isomerization. ChemCatChem 6(3):832–841. https://doi.org/10.1002/cctc.201300824
51. Hansford RC (1947) Mechanism of catalytic cracking. Ind Eng Chem 39(7):849–852. https://doi.org/10.1021/ie50451a012
52. Thomas CL (1949) Chemistry of cracking catalysts. Ind Eng Chem 41(11):2564–2573. https://doi.org/10.1021/ie50479a042
53. Tamele MW (1950) Chemistry of the surface and the activity of alumina-silica cracking catalyst. Discuss Faraday Soc 8:270–279. https://doi.org/10.1039/DF9500800270
54. Xu B, Sievers C, Lercher JA, van Veen JAR, Giltay P, Prins R, van Bokhoven JA (2007) Strong Brønsted acidity in amorphous silica–aluminas. J Phys Chem C 111(32):12075–12079. https://doi.org/10.1021/jp073677i
55. Poduval DG, van Veen JAR, Rigutto MS, Hensen EJM (2010) Bronsted acid sites of zeolitic strength in amorphous silica-alumina. Chem Commun 46(20):3466–3468. https://doi.org/10.1039/C000019A
56. Hensen EJM, Poduval DG, Degirmenci V, Ligthart DAJM, Chen W, Maugé F, Rigutto MS, van Veen JAR (2012) Acidity characterization of amorphous silica-alumina. J Phys Chem C 116(40):21416–21429. https://doi.org/10.1021/jp309182f
57. Crépeau G, Montouillout V, Vimont A, Mariey L, Cseri T, Maugé F (2006) Nature, structure and strength of the acidic sites of amorphous silica alumina: an IR and NMR study. J Phys Chem B 110(31):15172–15185. https://doi.org/10.1021/jp062252d
58. Huang J, van Vegten N, Jiang Y, Hunger M, Baiker A (2010) Increasing the Brønsted acidity of flame-derived silica/alumina up to zeolitic strength. Angew Chem Int Ed 49(42):7776–7781. https://doi.org/10.1002/anie.201003391
59. Xiong G, Elam JW, Feng H, Han CY, Wang HH, Iton LE, Curtiss LA, Pellin MJ, Kung M, Kung H, Stair PC (2005) Effect of atomic layer deposition coatings on the surface structure of anodic aluminum oxide membranes. J Phys Chem B 109(29):14059–14063. https://doi.org/10.1021/jp0503415
60. Verheyen E, Pulinthanathu Sree S, Thomas K, Dendooven J, De Prins M, Vanbutsele G, Breynaert E, Gilson JP, Kirschhock CEA, Detavernier C, Martens JA (2014) Catalytic activation of OKO zeolite with intersecting pores of 10- and 12-membered rings using atomic layer deposition of aluminium. Chem Commun 50(35):4610–4612. https://doi.org/10.1039/C3CC49028A
61. Puurunen RL (2005) Surface chemistry of atomic layer deposition: a case study for the trimethylaluminum/water process. J Appl Phys 97(12):121301. https://doi.org/10.1063/1.1940727
62. Wind RA, George SM (2009) Quartz crystal microbalance studies of Al2O3 atomic layer deposition using trimethylaluminum and water at 125 & #xB0;C. J Phys Chem A 114(3):1281–1289. https://doi.org/10.1021/jp9049268
63. Lakomaa EL, Root A, Suntola T (1996) Surface reactions in Al_2O_3 growth from trimethylaluminium and water by atomic layer epitaxy. Appl Surf Sci 107:107–115. https://doi.org/10.1016/S0169-4332(96)00513-2
64. Puurunen RL, Root A, Haukka S, Iiskola EI, Lindblad M, Krause AOI (2000) IR and NMR study of the chemisorption of ammonia on trimethylaluminum-modified silica. J Phys Chem B 104(28):6599–6609. https://doi.org/10.1021/jp000454i
65. Sree SP, Dendooven J, Koranyi TI, Vanbutsele G, Houthoofd K, Deduytsche D, Detavernier C, Martens JA (2011) Aluminium atomic layer deposition applied to mesoporous zeolites for acid catalytic activity enhancement. Catal Sci Technol 1(2):218–221. https://doi.org/10.1039/C0CY00056F
66. Zemtsova EG, Arbenin AY, Plotnikov AF, Smirnov VM (2015) Pore radius fine tuning of a silica matrix (MCM-41) based on the synthesis of alumina nanolayers with different thicknesses by atomic layer deposition. J Vac Sci Technol, A 33(2):021519. https://doi.org/10.1116/1.4907989
67. Feng H, Lu J, Stair P, Elam J (2011) Alumina over-coating on Pd nanoparticle catalysts by atomic layer deposition: enhanced stability and reactivity. Catal Lett 141(4):512–517. https://doi.org/10.1007/s10562-011-0548-8
68. Lu J, Elam JW, Stair PC (2013) Synthesis and stabilization of supported metal catalysts by atomic layer deposition. Acc Chem Res 46(8):1806–1815. https://doi.org/10.1021/ar300229c
69. Mäki-Arvela P, Hájek J, Salmi T, Murzin DY (2005) Chemoselective hydrogenation of carbonyl compounds over heterogeneous catalysts. Appl Catal A 292(1–2):1–49. https://doi.org/10.1016/j.apcata.2005.05.045
70. Yuan Y, Yao S, Wang M, Lou S, Yan N (2013) Recent progress in chemoselective hydrogenation of α, β-unsaturated aldehyde to unsaturated alcohol over nanomaterials. Curr Org Chem 17(4):400–413. https://doi.org/10.1016/j.cattod.2011.1009.1016
71. Ji X, Niu X, Li B, Han Q, Yuan F, Zaera F, Zhu Y, Fu H (2014) Selective hydrogenation of cinnamaldehyde to cinnamal alcohol over platinum/graphene catalysts. ChemCatChem 6:3246–3253. https://doi.org/10.1002/cctc.201402573
72. Zhu Y, Zaera F (2014) Selectivity in the catalytic hydrogenation of cinnamaldehyde promoted by Pt/SiO_2 as a function of metal nanoparticle size. Catal Sci Technol 4(4):955–962. https://doi.org/10.1039/C3CY01051A
73. Claus P, Schimpf S, Schödel R, Kraak P, Mörke W, Hönicke D (1997) Hydrogenation of crotonaldehyde on Pt/TiO_2 catalysts: influence of the phase composition of titania on activity and intramolecular selectivity. Appl Catal A 165(1–2):429–441. https://doi.org/10.1016/S0926-860X(97)00224-X
74. Kijeński J, Winiarek P, Paryjczak T, Lewicki A, Mikołajska A (2002) Platinum deposited on monolayer supports in selective hydrogenation of furfural to furfuryl alcohol. Appl Catal A 233(1–2):171–182. https://doi.org/10.1016/S0926-860X(02)00140-0
75. Weng Z, Zaera F (2018) Sub-monolayer control of mixed-oxide support composition in catalysts via atomic layer deposition: selective hydrogenation of cinnamaldehyde promoted by $(SiO_2$-ALD)-Pt/Al_2O_3. ACS Catal 8:8513–8524. https://doi.org/10.1021/acscatal.8b02431
76. Tiznado H, Fuentes S, Zaera F (2004) Infrared study of CO adsorbed on Pd/Al_2O_3-ZrO_2. Effect of zirconia added by impregnation. Langmuir 20(24):10490–10497. https://doi.org/10.1021/la049606h
77. Li Y, Zaera F (2015) Sensitivity of the glycerol oxidation reaction to the size and shape of the platinum nanoparticles in Pt/SiO_2 catalysts. J Catal 326:116–126. https://doi.org/10.1016/j.jcat.2015.04.009
78. Barrett EP, Joyner LG, Halenda PP (1951) The determination of pore volume and area distributions in porous substances I computations from nitrogen isotherms. J Am Chem Soc 73(1):373–380. https://doi.org/10.1021/ja01145a126
79. Groner MD, Fabreguette FH, Elam JW, George SM (2004) Low-temperature Al_2O_3 atomic layer deposition. Chem Mater 16(4):639–645. https://doi.org/10.1021/cm0304546
80. Cassidy DE, DeSisto WJ (2012) atomic layer deposition-modified ordered mesoporous silica membranes. Chem Vap Deposition 18(1–3):22–26. https://doi.org/10.1002/cvde.201106931

81. Gallezot P, Richard D (1998) Selective hydrogenation of α, β-unsaturated aldehydes. Catal Rev-Sci Technol 40(1–2):81–126. https://doi.org/10.1080/01614949808007106
82. Zaera F (2017) The surface chemistry of metal-based hydrogenation catalysis. ACS Catal 7:4947–4967. https://doi.org/10.1021/acscatal.7b01368
83. Giroir-Fendler A, Richard D, Gallezot P (1988) Selectivity in cinnamaldehyde hydrogenation of group-Viii metals supported on graphite and carbon. In: Guisnet M, Barrault J, Bouchoule C, Duprez D, Montassier C, Pérot G (eds) Studies in surface science and catalysis, vol 41. Elsevier, Amsterdam, pp 171–178
84. Ponec V (1997) On the role of promoters in hydrogenations on metals; α, β-unsaturated aldehydes and ketones. Appl Catal A 149(1):27–48. https://doi.org/10.1016/S0926-860X(96)00250-5
85. Claus P (1998) Selective hydrogenation of α, β-unsaturated aldehydes and other C=O and C=C bonds containing compounds. Top Catal 5(1–4):51–62. https://doi.org/10.1023/A:1019177330810
86. Schoenbaum CA, Schwartz DK, Medlin JW (2014) Controlling the surface environment of heterogeneous catalysts using self-assembled monolayers. Acc Chem Res 47(4):1438–1445. https://doi.org/10.1021/ar500029y
87. Arai M, K-i Usui, Nishiyama Y (1993) Preparation of alumina-supported platinum catalyst at ambient temperature for selective synthesis of cinnamyl alcohol by liquid-phase cinnamaldehyde hydrogenation. J Chem Soc, Chem Commun 24:1853–1854. https://doi.org/10.1039/C39930001853
88. Arai M, Obata A, Usui K, Shirai M, Nishiyama Y (1996) Activity for liquid-phase hydrogenation of α, β-unsaturated aldehydes of supported platinum catalysts prepared through low-temperature reduction. Appl Catal A 146(2):381–389. https://doi.org/10.1016/S0926-860X(96)00188-3
89. Zaki MI, Hasan MA, Al-Sagheer FA, Pasupulety L (2001) In situ FTIR spectra of pyridine adsorbed on SiO_2–Al_2O_3, TiO_2, ZrO_2 and CeO_2: general considerations for the identification of acid sites on surfaces of finely divided metal oxides. Colloids Surf A 190(3):261–274. https://doi.org/10.1016/S0927-7757(01)00690-2
90. Derouane EG, Védrine JC, Pinto RR, Borges PM, Costa L, Lemos MANDA, Lemos F, Ribeiro FR (2013) The Acidity of zeolites: concepts, measurements and relation to catalysis: a review on experimental and theoretical methods for the study of zeolite acidity. Catal Rev 55(4):454–515. https://doi.org/10.1080/01614940.2013.822266
91. Phung TK, Lagazzo A, Rivero Crespo MÁ, Sánchez Escribano V, Busca G (2014) A study of commercial transition aluminas and of their catalytic activity in the dehydration of ethanol. J Catal 311:102–113. https://doi.org/10.1016/j.jcat.2013.11.010
92. Parry EP (1963) An infrared study of pyridine adsorbed on acidic solids. Characterization of surface acidity. J Catal 2(5):371–379. https://doi.org/10.1016/0021-9517(63)90102-7
93. Hughes TR, White HM (1967) A study of the surface structure of decationized Y zeolite by quantitative infrared spectroscopy. J Phys Chem 71(7):2192–2201. https://doi.org/10.1021/j100866a035
94. Liu X (2008) Drifts study of surface of Γ-Alumina and its dehydroxylation. J Phys Chem C 112(13):5066–5073. https://doi.org/10.1021/jp711901s
95. Dong Y, Zaera F (2018) Selectivity in hydrogenation catalysis with unsaturated aldehydes: parallel versus sequential steps. J Phys Chem Lett 9:1301–1306. https://doi.org/10.1021/acs.jpclett.8b00173